

## Nonlinear theory of the photomagnetolectric effect with a quadratic relationship between carrier densities: Light intensity dependence

V. Augelli and L. Vasanelli

*Istituto di Fisica dell'Università di Bari, Bari, Italy*

*and Gruppo Nazionale di Struttura della Materia del Consiglio Nazionale delle Ricerche, Unità di Bari, Bari, Italy*

M. Leo, R. A. Leo, and G. Soliani

*Istituto di Fisica dell'Università di Lecce, Lecce, Italy*

(Received 19 May 1980)

A theory of the photomagnetolectric (PME) effect in the presence of a recombination mechanism, which involves a quadratic relationship between the carrier densities, is developed. Analytical expressions of PME short-circuit current ( $I_{\text{PME}}$ ) and photoconductance ( $\Delta G$ ) are found by solving the nonlinear continuity equation, in the case in which the light is strongly absorbed on the front surface of the sample. The power law of  $I_{\text{PME}}$  versus the light intensity is quadratic for high values of surface-recombination velocity and becomes linear for low values of this parameter. Similarly, the photoconductance has a linear dependence on light intensity for high surface-recombination velocities and a sublinear one for lower values of this last quantity. In all cases the  $I_{\text{PME}}$ -vs- $\Delta G$  behavior shows a quadratic power law. Finally, the dependence of  $I_{\text{PME}}$  and  $\Delta G$  on the parameters of the recombination model is discussed.

### I. INTRODUCTION

The photomagnetolectric (PME) effect has been extensively studied by many authors.<sup>1-4</sup> Various simplifying assumptions have been made in most cases in order to linearize the continuity equation. The carrier lifetimes and the ambipolar diffusion coefficient are generally assumed constants and the injection level is either very low or very high. In these cases the continuity equation is linear, and analytical expressions of the PME short-circuit current and photoconductance have been found.

Some authors<sup>5,6</sup> explained experimental data in the intermediate injection range by introducing particular models correlated to recombination and trapping processes acting in the investigated material. In this and following papers we will develop a more general theory of the PME effect which will take into account the recombination mechanism occurring in the material, without introducing hypotheses which allow one to linearize the continuity equation.

For any recombination model, functional relationships between the free-carrier concentrations  $n$  and  $p$ , and among these and the carrier recombination rate  $F$  can be calculated. These relationships generally lead to a nonlinear continuity equation, which is often very difficult to solve. Among the models more frequently used for the analysis of photoconductivity measurements, we have selected the case in which there is a quadratic relationship between  $p$  and  $n$ . In this particular case the nonlinear continuity equation can be solved and analytical expressions for

the PME short-circuit current and photoconductance can also be obtained. In Sec. II, the theory for the above-mentioned case is developed and in Sec. III, the behavior of the  $I_{\text{PME}}$  and  $\Delta G$  versus the light intensity is discussed.

### II. THEORY

#### A. Fundamental equations

The carrier transport through a semiconductor in the presence of magnetic and electric fields is described by the following continuity equations in steady-state conditions:

$$-F + \frac{1}{q} \vec{\nabla} \cdot \vec{J}_n + g(x, y, z; t) = 0, \quad (1)$$

$$-F - \frac{1}{q} \vec{\nabla} \cdot \vec{J}_p + g(x, y, z; t) = 0, \quad (2)$$

where  $q$  is the electronic charge,  $\vec{J}_n$  and  $\vec{J}_p$  are the electron- and hole-current densities, respectively,  $g(x, y, z; t)$  is the external pair generation rate. In the small Hall angle case, the general expressions of the current densities are

$$\vec{J}_n = \sigma_n \vec{E} + qD_n \vec{\nabla} n - \mu_n \vec{J}_n \times \vec{B}, \quad (3)$$

$$\vec{J}_p = \sigma_p \vec{E} - qD_p \vec{\nabla} p + \mu_p \vec{J}_p \times \vec{B}, \quad (4)$$

where  $\sigma_n$  and  $\sigma_p$  are the electron and hole conductivities,  $\vec{E}$  and  $\vec{B}$  the electric and magnetic fields,  $D_n$  and  $D_p$  the electron- and hole-diffusion coefficients, and  $\mu_n$  and  $\mu_p$  the electron and hole mobilities.

In the following we will assume (1) a semiconductor slab infinite in both  $x$  and  $z$  directions,

$x$  being the direction of the PME and photoconductivity currents,  $y$  and  $z$  those of the incident light and of the magnetic field, respectively; (2) a steady-state condition. With these hypotheses, we can write the  $y$  component of the electron current density as

$$J_{ny} = qD \frac{dn}{dy}, \quad (5)$$

where  $D$ , the generalized diffusivity function, is defined by:

$$D \equiv D_n \left( p + n \frac{dp}{dn} \right) / (p + bn), \quad (6)$$

where  $n$  and  $p$  are the free-carrier concentrations, and  $b$  is the electron-hole mobility ratio.

Since with our hypotheses  $\nabla \cdot \mathbf{J}_n = dJ_{ny}/dy$ , the continuity equation (1) can be rewritten as

$$-F + \frac{1}{q} \frac{dJ_{ny}}{dy} + g(x, y, z; t) = 0. \quad (7)$$

Furthermore, the following boundary conditions must be imposed:

$$Q_1 + D \frac{dn}{dy} \Big|_{y=0} = s_1 \Delta n(0) \quad \text{at } y=0, \quad (8)$$

$$Q_2 - D \frac{dn}{dy} \Big|_{y=w} = s_2 \Delta n(w) \quad \text{at } y=w, \quad (9)$$

where  $Q_1$  and  $Q_2$  are the generation rates on the front and back surfaces, respectively,  $s_1$  and  $s_2$  the corresponding surface recombination velocities,  $\Delta n$  is the excess carrier concentration, and  $w$  the sample thickness.

The solution of Eq. (7) under the boundary conditions (8) and (9) gives the carrier distribution in the sample. Then the short-circuit current per unit width  $I_{PME}$  and the photoconductance per unit width to length ratio  $\Delta G$  can be calculated by the following expressions:

$$I_{PME} = -B(\mu_n + \mu_p) \int_0^w J_{ny} dy, \quad (10)$$

$$\Delta G = q \int_0^w (\mu_n \Delta n + \mu_p \Delta p) dy. \quad (11)$$

### B. Nonlinear continuity equation

In the following, we will specialize Eqs. (7)–(9) to the case in which the light is absorbed at the front surface of the sample. Then we will assume the bulk recombination rate  $g(x, y, z; t) = 0$ , the surface generation rates  $Q_2 = 0$  and  $Q_1 = Q = \eta I(1 - R)$ , where  $\eta$  is the quantum efficiency,  $I$  the photon current density, and  $R$  the reflectivity.

If one assumes some model in order to describe the recombination mechanism of the charge carriers,

the rate equations for the steady state allow one to obtain a relationship between  $p$  and  $n$  and another one between the generation rate  $F$  and  $p$  and  $n$ ,  $F = F(p, n)$ . Generally, the relationship between  $p$  and  $n$  is in implicit form and only in some particular cases can it be solved so as to express  $p$  as a function of  $n$ . Then,  $F$  can be written as a function of  $n$  and therefore Eqs. (5)–(7) give a differential equation whose solution is the charge carrier distribution  $n(y)$ . Generally, this differential equation is nonlinear and very hard to solve. In this paper, we will deal with the problem of the determination of the charge-carrier distribution in the case where

$$p = A n^2 \quad (12)$$

and

$$F = C n^2. \quad (13)$$

The physical meaning of the constants  $A$  and  $C$ , in a simple model, is discussed in Appendix A.

These relationships have been widely used to describe the photoconductivity behavior in many experimental cases,<sup>7</sup> both for insulators and semiconductors providing that the injection level is high enough. In the following we will assume that intermediate or high injection condition is verified, i.e.,  $\Delta n \approx n$ ,  $\Delta p \approx p$ .

Taking into account Eq. (6), the continuity equation (7) can be rewritten, through Eqs. (12) and (13), as

$$-Cn^2 + 3AD_n \frac{d}{dy} \left( \frac{n}{An+b} \frac{dn}{dy} \right) = 0. \quad (14)$$

Equation (14) cannot be solved analytically; however, if one considers two different ranges in which  $n$  can vary, so that either  $An \ll b$  or  $An \gg b$ , two different analytical solutions can be found. In this paper we deal with the case  $An \ll b$ .<sup>8</sup> Thus, Eq. (14) becomes

$$-\frac{bC}{3AD_n} n^2 + \left( \frac{dn}{dy} \right)^2 + n \frac{d^2 n}{dy^2} = 0. \quad (15)$$

Equation (15) can be readily linearized by putting

$$n(y) = [u(y)]^{1/2}. \quad (16)$$

In doing so, we obtain:

$$\frac{d^2 u}{dy^2} - \frac{1}{L^{*2}} u = 0, \quad (17)$$

where  $L^{*2} = 3AD_n/2bC$ . Thus, the general solution of Eq. (15) is easily found and is given by

$$n(y) = (c_1 e^{y/L^*} + c_2 e^{-y/L^*})^{1/2}, \quad (18)$$

where  $c_1$  and  $c_2$  are integration constants to be determined through the boundary conditions, Eqs. (8) and (9). We must observe that the quantity

$L^*$  plays the same role as the diffusion length in the standard linear theory. In the next section we will show that  $L^*$  is closely related to the hole-carrier diffusion length.

In what follows, we will use the following dimensionless quantities:

$$Y = \frac{y}{L^*}, \quad W = \frac{w}{L^*}, \quad S_1 = \frac{s_1 w}{3D_p}, \quad S_2 = \frac{s_2 w}{3D_p}. \quad (19)$$

Also, it is convenient to introduce the quantity

$$Q^* = \frac{Qw}{3D_p}. \quad (20)$$

The boundary conditions, Eqs. (8) and (9), can be rewritten by using these quantities as

$$\frac{1}{A} \frac{Q}{W} + n \frac{dn}{dY} \Big|_{Y=0} = \frac{1}{A} \frac{S_1}{W} n(0), \quad (21)$$

$$-n \frac{dn}{dY} \Big|_{Y=W} = \frac{1}{A} \frac{S_2}{W} n(W). \quad (22)$$

The short-circuit PME current can be derived from Eq. (10) and its analytical expression results:

$$I_{PME} = -qw^2 B (\mu_n + \mu_p) \frac{C}{W^2} [C_1(e^W - 1) + C_2(e^{-W} - 1)]. \quad (23)$$

Since in our model,  $\Delta n \approx n$ ,  $\Delta p \approx p$ , the photoconductance is given by [see Eqs. (11), (12), and (18)]

$$\Delta G = qw \mu_n \left( \frac{1}{W} \int_0^W n(Y) dY + \frac{A}{Wb} [C_1(e^W - 1) + C_2(1 - e^{-W})] \right). \quad (24)$$

The analytical expression of the integral is given in Appendix B.

### III. DISCUSSION

Before we discuss the behavior of  $I_{PME}$  and  $\Delta G$  as a function of the various parameters, it should be pointed out that the electron lifetime  $\tau_n$  is inversely proportional to the electron carrier concentration; in fact,

$$\tau_n \equiv \frac{\Delta n}{F} = \frac{1}{Cn}.$$

Moreover, the hole lifetime  $\tau_p$  is constant, being

$$\tau_p \equiv \frac{\Delta p}{F} = \frac{A}{C}.$$

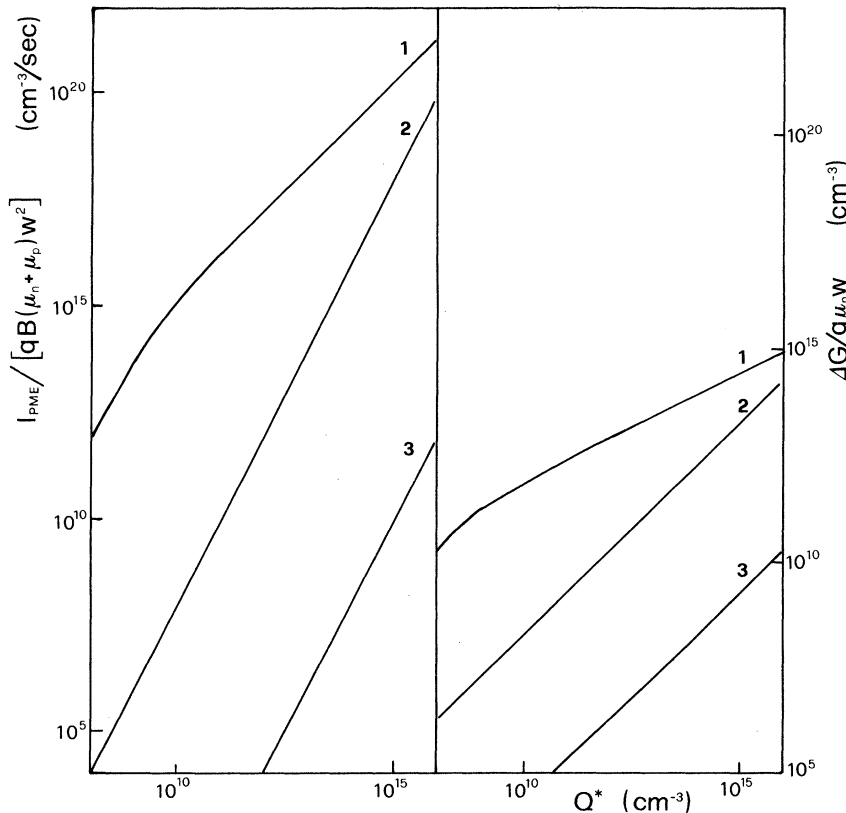


FIG. 1. The quantities  $I_{PME}/qB(\mu_n + \mu_p)w^2$  and  $\Delta G/q\mu_n w$  vs  $Q^*$ .  $A=10^{-16}$  cm<sup>3</sup>,  $W=10$ ,  $C=10^{-8}$  cm<sup>3</sup> sec<sup>-1</sup>,  $S_2=0$ . The curves 1, 2, 3 are obtained assuming  $S_1=10^{-3}$ ,  $10$ ,  $10^5$ , respectively.

Then the hole diffusion length  $L_p$  is constant and related to the quantity  $L^*$ , introduced in Eq. (17), by

$$L_p = \sqrt{2/3} L^*.$$

In Fig. 1,  $I_{PME}/qB(\mu_n + \mu_p)w^2$  and  $\Delta G/q\mu_n w$  are plotted as a function of the quantity  $Q^*$  related to the light intensity by Eq. (20). The curves have been computed for a case in which  $A = 10^{-16} \text{ cm}^3$ ,  $W = 10$ ,  $S_2 = 0$ ,  $C = 10^{-8} \text{ cm}^3 \text{ sec}^{-1}$ , and for different values of  $S_1$ . The investigated range of light intensity has been selected so that the condition  $An \ll b$  is always satisfied. As one can see, the magnitude of  $I_{PME}$  and  $\Delta G$  increases as the front-surface recombination velocity decreases.

The  $I_{PME}$  and  $\Delta G$ -vs- $Q^*$  curves, plotted on a log-log scale, have slopes equal to 2 and 1, respectively, for high surface-recombination velocities. For a lower  $S_1$  value, there is a decrease in the slope, down to 1 for the  $I_{PME}$  curve and 0.5 for  $\Delta G$ .

Moreover, if the pairs of  $I_{PME}$  and  $\Delta G$  values, deduced from each pair of curves in Fig. 1, are plotted in a log-log plot (Fig. 2), a single straight line is obtained. The slope of this line is 2, and therefore it is clearly independent of  $S_1$ . Different values of  $S_1$  determine the region on the line where the pairs of  $I_{PME}$  and  $\Delta G$  values are situated.

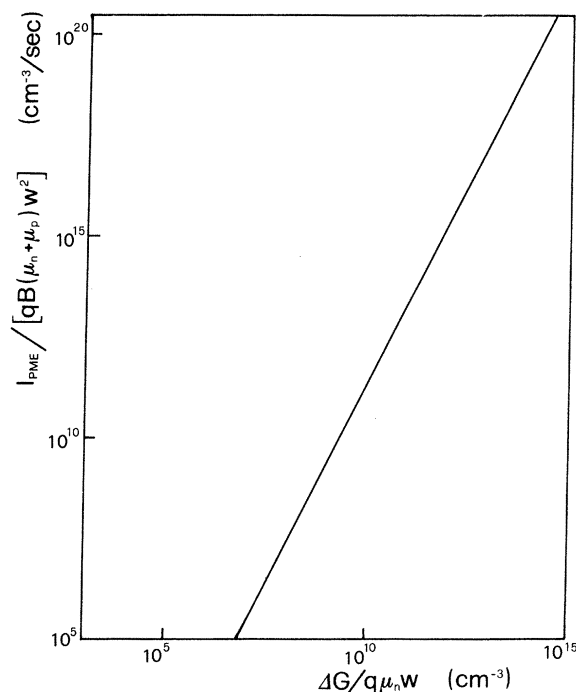


FIG. 2. PME short-circuit current versus photoconductance. The values of the parameters are the same as in Fig. 1.

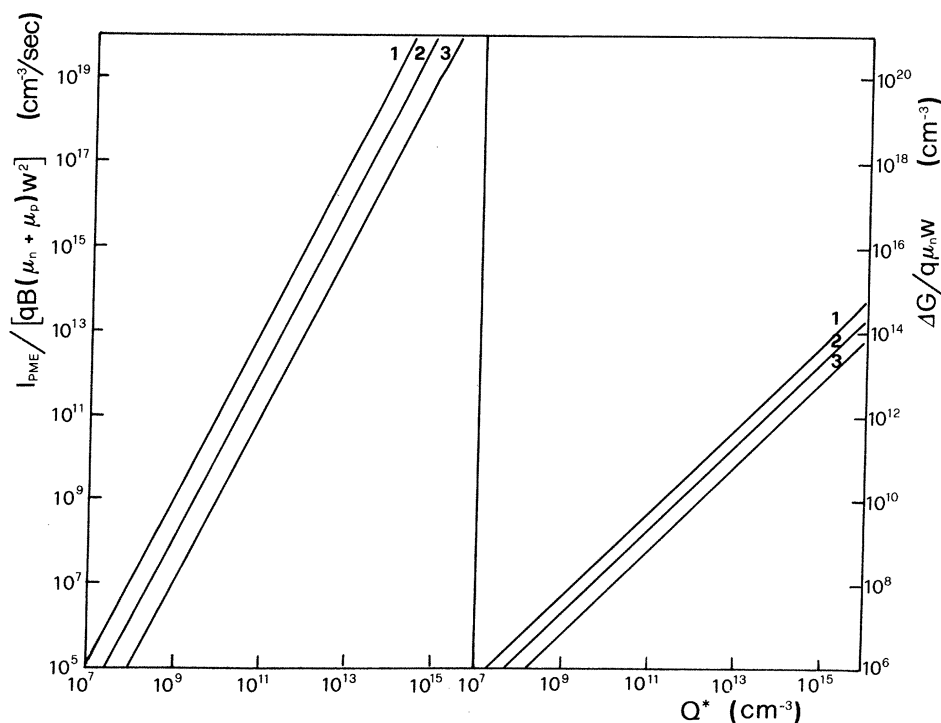


FIG. 3. PME short-circuit current and photoconductance versus  $Q^*$ .  $C = 10^{-8} \text{ cm}^3 \text{ sec}^{-1}$ ,  $S_1 = 10$ ,  $S_2 = 0$ . Curve 1:  $A = 10^{-15} \text{ cm}^3$ ,  $W = 3.2$ . Curve 2:  $A = 10^{-16} \text{ cm}^3$ ,  $W = 10$ . Curve 3:  $A = 10^{-17} \text{ cm}^3$ ,  $W = 32$ .

Figure 3 shows the  $I_{\text{PME}}$  and  $\Delta G$  vs  $Q^*$  with  $A$  as a parameter. The curves have been calculated with  $S_1=10$ ,  $S_2=0$ , and  $C=10^{-8} \text{ cm}^3 \text{ sec}^{-1}$ . In order to analyze the  $I_{\text{PME}}$  and  $\Delta G$  behavior under the same condition, it must be kept in mind that  $W$  and  $A$  are related by the following expression:

$$W = w(3AD_n/2bc)^{-1/2}. \quad (25)$$

Thus  $W$  assumes different values as  $A$  varies.

Two remarks can be made about the curves shown in Fig. 3. The first is that the slopes of both  $I_{\text{PME}}$  and  $\Delta G$  plots are unaffected by the magnitude of  $A$ ; the second is that the magnitude of both  $I_{\text{PME}}$  and  $\Delta G$  increases as  $A$  does. Applying this result to the example reported in Appendix A, one finds that  $I_{\text{PME}}$  and  $\Delta G$  values decrease as the recombination center concentration increases.

Figure 4 is the plotted curves of  $I_{\text{PME}}$  and  $\Delta G$  vs  $Q^*$  for three different values of the parameter  $C$ . These curves have been computed assuming  $A=10^{-16} \text{ cm}^3$ ,  $S_1=10$ ,  $S_2=0$ , and  $W$  changes with  $C$  according to Eq. (25). As one can see, the  $I_{\text{PME}}$  current is independent of  $C$ , as is evident from Eq. (23), while  $\Delta G$  decreases as  $C$  increases.

In conclusion, the theoretical analysis of the  $I_{\text{PME}}$  and  $\Delta G$  behavior as a function of the light

intensity shows, as a peculiar feature, a quadratic power law between  $I_{\text{PME}}$  and  $\Delta G$  in the range in which  $p \propto n^2$  and  $An \ll b$ .

This result disagrees with that reported in Ref. 5 obtained by assuming a similar model but a constant electron recombination lifetime. The dependence of  $I_{\text{PME}}(\Delta G)$  on the light intensity is generally quadratic (linear). For a low surface-recombination velocity, the slope of the  $I_{\text{PME}}$ -vs- $Q^*$  curve, changes from superlinear to linear, while that of the  $\Delta G$ -vs- $Q^*$  curve becomes 0.5. The values of the parameter  $A$  affect the magnitude of both  $I_{\text{PME}}$  and  $\Delta G$ , while the parameter  $C$  affects only the magnitude of  $\Delta G$ .

#### ACKNOWLEDGMENT

This work was partially supported by the Consiglio Nazionale delle Ricerche, Italy, and in part by the Istituto Nazionale di Fisica Nucleare.

#### APPENDIX A

In this appendix, we report an application of our model, as an example. Let us consider a situation in which the recombination kinetics are controlled by two levels, as shown in Fig. 5. Center 1 plays

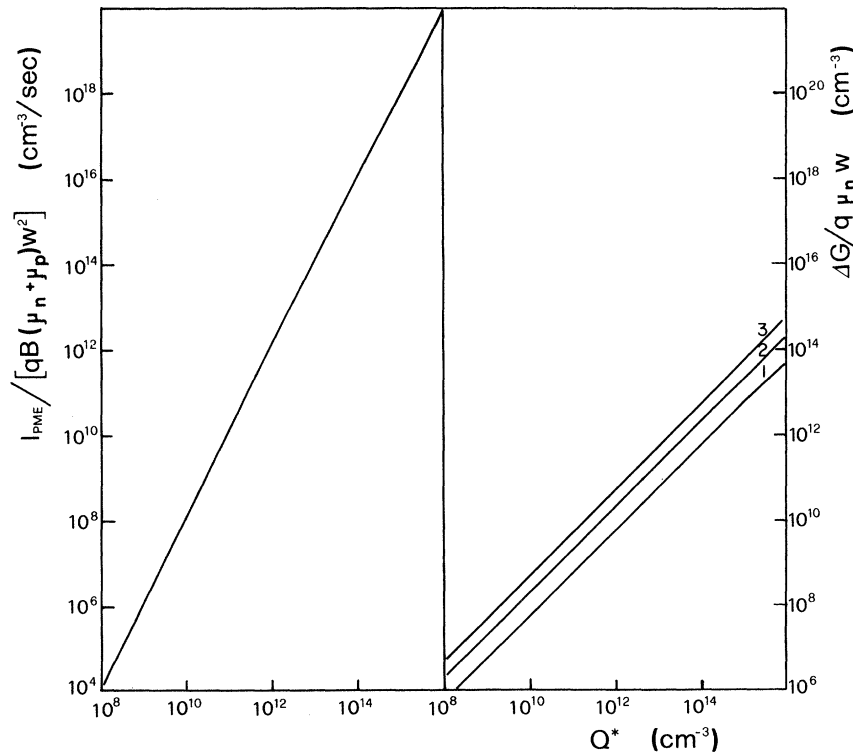


FIG. 4. PME short-circuit current and photoconductance versus  $Q^*$ .  $A=10^{-16} \text{ cm}^3$ ,  $S_1=10$ ,  $S_2=0$ . Curve 1:  $C=10^{-7} \text{ cm}^3 \text{ sec}^{-1}$ ,  $W=32$ . Curve 2:  $C=10^{-8} \text{ cm}^3 \text{ sec}^{-1}$ ,  $W=10$ . Curve 3:  $C=10^{-9} \text{ cm}^3 \text{ sec}^{-1}$ ,  $W=3.2$ . The  $I_{\text{PME}}$  curve is unaffected by the parameter  $C$ .

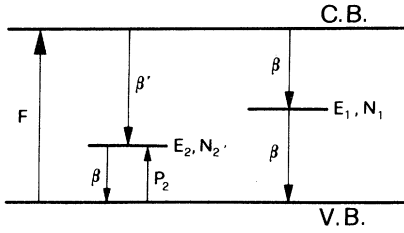


FIG. 5. Energy-level scheme, showing position, density, capture probability, and thermal-excitation probability of the centers.

the role of recombination center, while level 2 is a hole-trapping center.

The rate equations for the steady state are

$$F = \beta n (N_1 - n_1) + \beta' n (N_2 - n_2), \quad (\text{A1})$$

$$0 = \beta' n (N_2 - n_2) - \beta p n_2 + P_2 (N_2 - n_2), \quad (\text{A2})$$

$$0 = \beta n (N_1 - n_1) - \beta p n_1, \quad (\text{A3})$$

where  $n_1$  and  $n_2$  are the densities of the centers occupied by electrons at  $E_1$  and  $E_2$ , respectively,  $P_2 = N_v e^{(E_v - E_2)/kT}$  is the probability for thermal excitation of holes from centers at  $E_2$  to the valence band, and the other symbols have the standard meaning. The charge neutrality condition

$$n = p + (N_1 - n_1) + (N_2 - n_2) \quad (\text{A4})$$

must also be taken into account. Let us discuss the case in which level 2 lies under both the hole Fermi level and the hole demarcation level, and  $\beta'$  is much less than  $\beta$ . In the injection range where  $\beta N_2 n \ll P_2 N_1$ , and  $4n^2(P_2 + \beta N_2) \ll P_2 N_1^2$ , one can easily obtain the following relationship between the charge-carrier concentrations:

$$p \approx n^2/N_1. \quad (\text{A5})$$

Comparison between Eqs. (A5) and (12) shows that the constant  $A$  is equal to the inverse of the recombination-center concentration. The hypotheses made imply that the injection range in which Eq. (A5) is valid, is limited by two conditions:

$$n \ll \frac{N_1 N_2}{N_2} e^{-E_2/kT}, \quad (\text{A6})$$

$$n \ll N_1.$$

Figure 6 shows two  $p$ -vs- $n$  curves, calculated for our model by Eq. (A4) with different values of  $E_2$  and  $N_2$ . It is clearly shown that there is a wide range of electron concentrations where Eq. (A5) is suitable to describe the carrier densities in agreement with the limiting conditions (A6). Furthermore, the condition  $An \ll b$  used to solve the nonlinear continuity equation is quite satisfied because  $b$  generally ranges between 1 and 100.

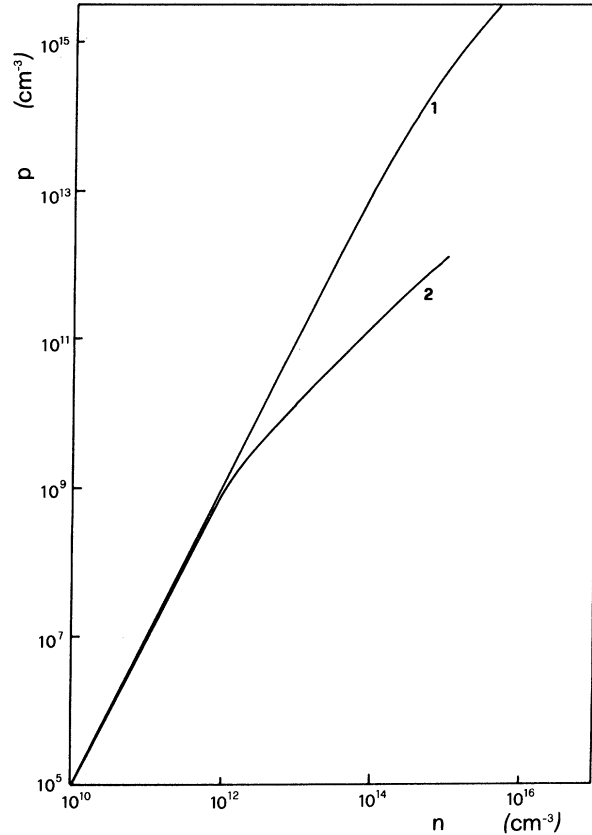


FIG. 6.  $p$ -vs- $n$  plot. Curve 1:  $E_2 = 0.1$  eV,  $N_2 = 10^{17}$   $\text{cm}^{-3}$ ,  $N_1 = 10^{15}$   $\text{cm}^{-3}$ . Curve 2:  $E_2 = 0.4$  eV,  $N_1 = N_2 = 10^{15}$   $\text{cm}^{-3}$ .

With the previous assumptions, the recombination rate  $F$  is given by

$$F \approx \beta n^2. \quad (\text{A7})$$

Then in this case the constant  $C$  of Eq. (13) is just the capture probability  $\beta$ . These relationships are easily obtained for the insulating materials; for semiconductors, Eqs. (A5) and (A7) are still valid providing that  $\Delta n \gg n_0$ .

#### APPENDIX B

The integral

$$g = \int_0^w n(Y) dY, \quad (\text{B1})$$

which appears in Eq. (24), can be readily evaluated by noting that

$$n^2(Y) = C_1 e^Y + C_2 e^{-Y} = C' \cosh(Y + \delta), \quad (\text{B2})$$

where

$$C' = 2\sqrt{C_1 C_2}, \quad \frac{C_1 - C_2}{C_1 + C_2} = \tanh \delta.$$

Then, substituting (B2) in (B1) and performing

the change of variable  $Y=2x-\delta$ , we obtain the expression (see Ref. 9, p. 115)

$$g = 2\sqrt{C'} \left\{ \frac{1}{\sqrt{2}} \left[ F\left(\theta_2, \frac{1}{\sqrt{2}}\right) - F\left(\theta_1, \frac{1}{\sqrt{2}}\right) \right] - \sqrt{2} \left[ E\left(\theta_2, \frac{1}{\sqrt{2}}\right) - E\left(\theta_1, \frac{1}{\sqrt{2}}\right) \right] + \frac{\sinh(W+\delta)}{[\cosh(W+\delta)]^{1/2}} - \frac{\sinh\delta}{\sqrt{\cosh\delta}} \right\},$$

where  $F$  and  $E$  are the elliptic integrals of the first and of the second kind, respectively,

$$\theta_2 = \arccos \frac{1 - \sinh(W+\delta)}{1 + \sinh(W+\delta)},$$

and

$$\theta_1 = \arccos \frac{1 - \sinh\delta}{1 + \sinh\delta}.$$

<sup>1</sup>W. van Roosbroeck, Phys. Rev. **101**, 1713 (1956).

<sup>2</sup>W. Gartner, Phys. Rev. **105**, 823 (1957).

<sup>3</sup>D. C. Look, Phys. Rev. B **16**, 5460 (1977).

<sup>4</sup>V. Augelli, C. Manfredotti, R. Murri, R. Piccolo, and L. Vasanelli, Phys. Rev. B **18**, 5484 (1978).

<sup>5</sup>J. Agraz-G. and S. S. Li, Phys. Rev. B **2**, 1847 (1970).

<sup>6</sup>S. S. Li and C. I. Huang, J. Appl. Phys. **43**, 1757 (1972).

<sup>7</sup>R. H. Bube, *Photoconductivity of Solids* (Wiley, New York, 1960), Chap. 11.

<sup>8</sup>The case  $An \gg b$  will be discussed in a forthcoming paper.

<sup>9</sup>I. S. Gradshteyn and I. M. Ryzhik, *Tables of Integrals, Series and Products* (Academic, New York, 1965).